Stem Cell Reports
Article
OPEN ACCESS

Origins of Neural Progenitor Cell-Derived Axons Projecting Caudally after Spinal Cord Injury

Paul Lu,[1,2,6,*] Walace Gomes-Leal,[2,3,6] Selin Anil,[2,4] Gabriel Dobkins,[2] J. Russell Huie,[5] Adam R. Ferguson,[5] Lori Graham,[2] and Mark Tuszynski[1,2,*]

[1]Veterans Administration-San Diego Healthcare System, San Diego, CA 92161, USA
[2]Department of Neurosciences, University of California, San Diego, La Jolla, CA 92093-0626, USA
[3]Laboratory of Experimental Neuroprotection and Neuroregeneration, Institute of Biological Sciences, Federal University of Pará Belém, Brazil
[4]Center for Neuroprosthetics and Brain Mind Institute, School of Life Sciences, Swiss Federal Institute of Technology (EPFL), Geneva, Switzerland
[5]Department of Neurological Surgery, University of California, San Francisco, San Francisco, CA, USA
[6]Co-first author
*Correspondence: plu@ucsd.edu (P.L.), mtuszynski@ucsd.edu (M.T.)
https://doi.org/10.1016/j.stemcr.2019.05.011

SUMMARY

Neural progenitor cells (NPCs) transplanted into sites of spinal cord injury (SCI) extend large numbers of axons into the caudal host spinal cord. We determined the precise locations of neurons in the graft that extend axons into the caudal host spinal cord using AAV9-Cre-initiated retrograde tracing into floxed-TdTomato-expressing NPC grafts. 7,640 ± 630 grafted neurons extended axons to a single caudal host spinal cord site located 2 mm beyond the lesion, 5 weeks post injury. While caudally projecting axons arose from neurons located in all regions of the graft, the majority of caudally projecting graft neurons (53%) were located within the caudal one-third of the graft. Numerous host corticospinal axons formed monosynaptic projections onto caudally projecting graft neurons; however, we find that the majority of host axonal neuronal projections formed by neural progenitor cell interneuronal "relays" across sites of SCI are likely polysynaptic in nature.

INTRODUCTION

Spinal cord injury (SCI) results in disruption of projections between rostral and caudal segments of the spinal cord. One strategy for potentially restoring synaptic connectivity between segments of the spinal cord rostral and caudal to the lesion is the implantation of neural progenitor cells (NPCs) or neural stem cells into the lesion site (Haas and Fischer, 2014); these stem cell grafts can form new neuronal relays across the lesion (Lu et al., 2012b, 2014, 2017). Implanted NPCs extend large numbers of axons for long distances into the host spinal caudal to the lesion, and host axons regenerate into the stem cell grafts (Lu et al., 2014, 2017, 2012b; Bonner et al., 2011; Kadoya et al., 2016; Rosenzweig et al., 2018); each of these new projections form synapses, and functional improvement is observed (Bonner et al., 2011; Kadoya et al., 2016; Koffler et al., 2018; Kumamaru et al., 2018; Lu et al., 2017, 2012b; Rosenzweig et al., 2018).

While novel relays appear to form across the lesion site based on electrophysiological evidence (Koffler et al., 2018; Lu et al., 2012b) and, indirectly, improved functional outcomes after complete spinal cord transection (Koffler et al., 2018; Lu et al., 2012b), little is known about the anatomical complexity of these relays. Host corticospinal motor axons regenerate distances of up to 1 mm into the 2- to-3 mm-long NPC grafts in the lesion site, and synapse onto graft neurons (Kadoya et al., 2016); in turn, graft-derived axons grow out from the lesion site for distances up to 50 mm into the caudal host spinal cord (Lu et al., 2014, 2017, 2012b; Rosenzweig et al., 2018). In this study, we sought to characterize the nature of host-to-graft-to-host connectivity across NPC grafts placed into sites of cervical spinal cord lateral hemisection. We used a combination of retrograde labeling initiated from the host spinal cord caudal to the NPC graft and anterograde labeling of host corticospinal axons regenerating into NPC grafts to determine whether evidence supports the probability that monosynaptic connections can form from host-to-graft-to-host across a site of SCI, or whether trans-graft connectivity is more likely to be polysynaptic in nature. It has been hypothesized that monosynaptic projections across grafts may be more efficient (Berry and Pentreath, 1976). We used highly sensitive AAV9-Cre-mediated retrograde labeling in mouse NPC grafts expressing Cre-dependent TdTomato, or retrograde Fluoro-Gold (FG) labeling in rat NPC grafts, to determine the nature of trans-synaptic connectivity in two different species. We now find that a combination of monosynaptic and polysynaptic projections likely contribute to re-establishment of trans-graft connectivity following NPC grafting.

RESULTS

Caudal Neurons in Mouse Neural Progenitor Cell Grafts Are the Source of Most Distal Projections to the Host Spinal Cord

Injections of AAV9-Cre into the host spinal cord 2 mm caudal to the site of grafting showed that AAV9-Cre

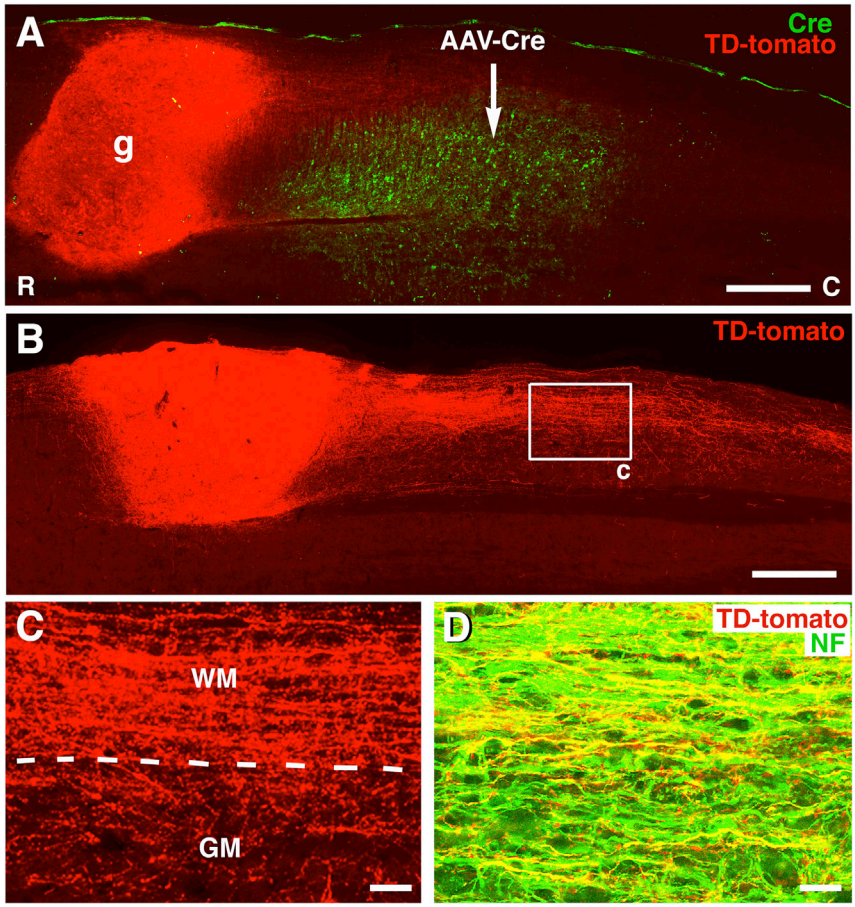

Figure 1. Retrograde Labeling of Caudally Projecting Neurons through Cre-Mediated Expression in TdTomato-Expressing Mouse Neural Progenitor Cell Grafts

Wild-type mice received grafts of NPCs expressing Cre-dependent TdTomato into a site of C5 hemisection, and injections of AAV9-Cre into the caudal host spinal cord 2 weeks later.

(A) Overview of one section double labeled for anti-TdTomato and anti-Cre to demonstrate position of AAV9-Cre injection (arrow) 2 mm caudal to NPC graft (g). Graft is from donor transgenic mouse E12 spinal cord that conditionally expresses TdTomato. Horizontal section, rostral to left. Graft occupies right C5 lateral hemisection lesion cavity. All TdTomato labeling in graft arises from cells in graft bearing axons that project to the caudal site of AAV9-Cre injection, since TdTomato expression is Cre dependent. Individual neurons in graft are shown in Figure 2.

(B) A different section from the same animal exhibits a large number of TdTomato-expressing axons extending from the graft into the caudal host spinal cord.

(C) Higher magnification of boxed area in (B). Axons extend through both white and gray matter. Dashed lines indicate border of white matter (WM) and gray matter (GM).

(D) Neurofilament-200 (NF), an axonal marker, and TdTomato are frequently co-expressed, indicating the axonal nature of TdTomato-labeled processes extending into the caudal host spinal cord. Image is 2 mm caudal from the graft.

Scale bars represent 550 μm (A), 530 μm (B), 63 μm (C), and 19 μm (D).

injections were locally restricted and did not spread directly into grafts (Figure 1A). Numerous neurons in the graft were labeled for TdTomato, generated by recombination of *loxP* sites resulting from distal AAV9-Cre injections into the host (Figures 1, 2, and 3). The expression of TdTomato in grafted neurons demonstrated the extension of very large numbers of axons form the grafts and into the caudal host spinal cord (Figures 1B and 1C). Notably, TdTomato-labeled axons grew from grafts exclusively in the caudal direction (Figures 1B and 1C). The axonal identity of TdTomato-expressing processes from grafts was confirmed by double labeling of all such extensions with neurofilament (NF) (Figure 1D). Accordingly, there was no TdTomato expression in glia.

Graft neurons that extended axons caudal to the lesion were located at all rostral-caudal levels of the graft based on TdTomato somal labeling, but with a marked preponderance for a caudal position (Figures 1 and 2). These TdTomato-labeled cells were of neuronal identity, based on exclusive co-localization with the neuronal marker NeuN (Figures 2C and 2D). Quantification revealed that a total of 7,640 ± 630 neurons per graft extended axons to the caudal site of AAV9-Cre expression, 2 mm below the lesion site. A continuous gradient of neurons extending axons caudal to the lesion site was found, with the greatest proportion of caudally projecting neurons present in caudal levels of the graft (quantified in Figure 2E). Indeed, 53% of neurons in the graft projecting to the caudal AAV9-Cre injection site were located within the caudal one-third of the graft (Figures 2E and 2F), and 78% of TdTomato-expressing neurons were present in the caudal one-half of the graft (Figures 2E and 2F). Only approximately 10% of neurons projecting axons to the caudal host spinal cord were located in the rostral one-third of the graft (Figures 2E and 2F). These data indicate that most caudally projecting neurons are located within caudal portions of the graft.

Inspection of individual TdTomato-labeled neurons in grafts demonstrated that neurites project out from grafted

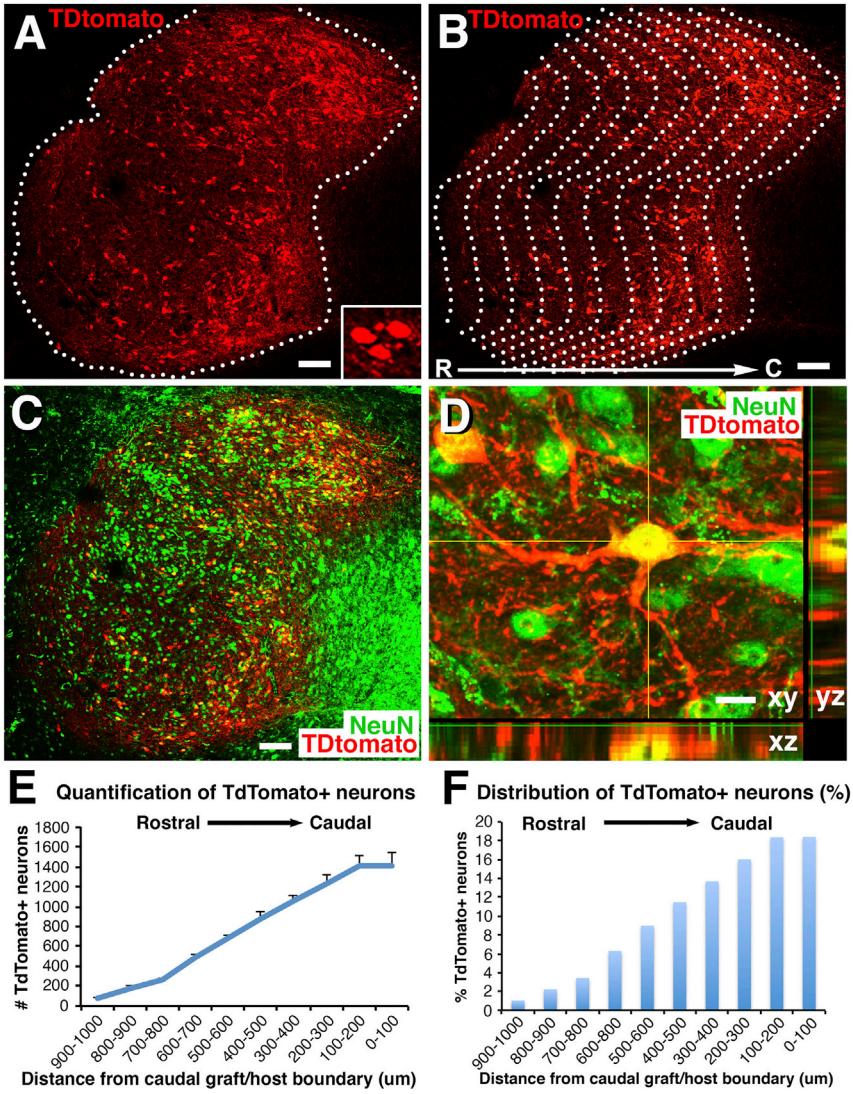

Figure 2. TdTomato Retrogradely Labeled Neurons in Mouse NPC Grafts

(A and B) TdTomato-labeled cells are located throughout the graft with the highest density in caudal regions of the graft. Rostral (R), left; caudal (C), right. Dashed lines outline the TdTomato-expressing graft. Inset in (A) shows small cluster of TdTomato-expressing cells. Note that the copied caudal border line is superimposed at 100-μm intervals (B) to divide the whole graft into a series of repeating 100-μm regions distributed from the caudal to rostral graft border, and cells on each 100-μm zone are quantified in (E) and (F). Scale bars, 128 μm.

(C) NeuN labeling of same section. All cells labeled for TdTomato also express NeuN. Scale bar, 128 μm.

(D) A z-stack confocal image showing co-localization of TdTomato and NeuN. Scale bar, 12 μm.

(E) Quantification the total number of TdTomato$^+$ neurons at each 100-μm interval from the rostral to caudal extent of the graft ($n = 5$). One-way ANOVA, $p < 0.0001$; post hoc Fisher's test shows significant differences in neuron number between each interval from 100–200 μm to 600–700 μm. The total mean number of retrogradely labeled neurons in this mouse NPC graft is 7,640 ± 630 cells. Error bars denote ±SEM.

(F) Distribution of TdTomato$^+$ neurons in each 100-μm interval as average percentage of total TdTomato$^+$ neurons along the rostrocaudal extent of the NPC graft. Approximately 50% of retrogradely labeled neurons in graft that project to the caudal spinal cord are located within the distal (caudal) one-third of the graft.

neurons radially in many directions (Figure 3A). Quantification demonstrated that the angles at which neurites emerged from grafted neurons was uniformly distributed around a 360° axis, with no statistically significant preferred direction of growth ($p = 0.92$, Rayleigh's test; Figure 3B). Moreover, there was no significant difference in mean angle of neurite emergence in neurites located in the rostral, middle, or caudal compartments of the graft ($p = 0.97$). Thus, there is no preference for neurites to emerge from grafted neurons in any particular orientation. Emergence of neurites in random directions from grafted neurons suggests that neurons located most caudally in grafts are more likely to extend axons into caudal host white matter, given the proximity of the caudally located neuron to these anatomically distal regions of the host.

Mouse Host Corticospinal Axons Can Form Monosynaptic Connections with Caudally Projecting Graft Neurons; Most Projections Are Likely Polysynaptic

To determine whether these caudally projecting graft neurons are capable of forming monosynaptic relays from host-to-graft-to-host across the lesion site, we examined the juxtaposition of host corticospinal tract (CST) terminals regenerating in grafts to TdTomato-expressing neurons (which, by virtue of TdTomato expression, must extend an axon to the host caudal to the lesion). GFP-expressing CST axons regenerated into NPC grafts and were primarily present within the rostral 500 μm of the graft (Figure 4A). In these regions, TdTomato-expressing graft neurons were present, and in several instances received direct CST axonal appositions onto the

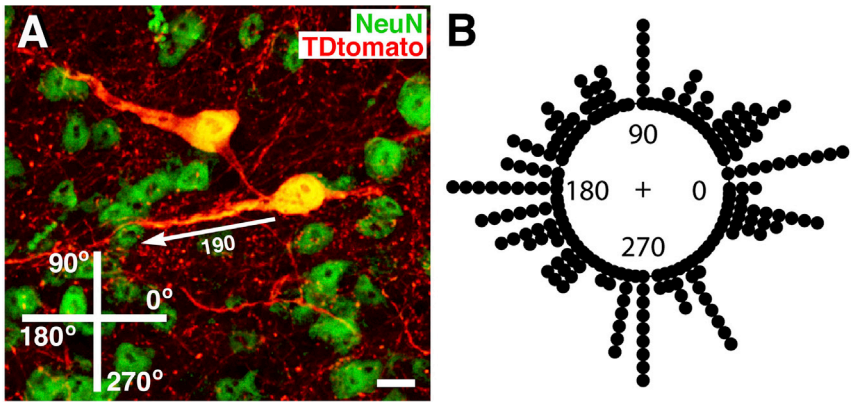

Figure 3. Orientation of Neurite Emergence from Grafted NPCs

(A) TdTomato and NeuN double labeling reveals the orientation of neurite emergence from grafted NPCs in the spinal cord lesion cavity. The angle of emergence was measured among 218 neurites. Scale bar, 15 μm.

(B) Angle of emergence of each neurite shown in circular histogram. The numbers on the inner edge of the circumference indicate the angle of neurite emergence. The circular mean is 283.93, and Rayleigh's test of uniformity shows that there is no significant deviation from uniform distribution ($p = 0.92$).

TdTomato-expressing cell soma (Figures 4B and 4C) and processes (Figures 4B and 4D). 3.9% ± 0.9% of TdTomato-expressing neurons in the graft received close appositional contacts from GFP-labeled host corticospinal axons. This number is mostly likely an underestimate of such contacts because those corticospinal axons that contacted TdTomato neurites rather than somata were not counted. Many of these CST axonal terminals that contacted TdTomato-expressing neurons exhibited bouton-like morphology and co-localized with the presynaptic marker synaptophysin (Figure 4E). Nearly all GFP-labeled terminal boutons co-expressed synaptophysin; an occasional bouton did not clearly co-localize with synaptophysin, which may have been a result of the synaptophysin immunoreactive product being out of the plane of section. Grafted neurons that extended axons into the caudal host spinal cord also formed bouton-like appositions with host neurons that co-localized with synaptophysin (Figure 4F). Thus, anatomical disynaptic connections from host-to-graft-to-host were present.

Most TdTomato-expressing neurons were located in the caudal one-half of the graft, beyond the distance to which most corticospinal axons regenerated. For these caudally projecting neurons in the graft, any relay of synaptic activity from host corticospinal axons to caudally projecting graft neurons would have to occur polysynaptically through graft "interneurons" rather than monosynaptically.

Rat Host Corticospinal Axons Can Form Monosynaptic Connections with Caudally Projecting Graft Neurons; Most Projections Are Likely Polysynaptic

We also examined whether there is a regional predominance among caudally projecting neurons in rat NPC grafts. Anatomical analyses demonstrated that grafts survived and filled the lesion site in five of six animals (Figure 5A); the sixth animal had incomplete graft fill at the caudal aspect of the lesion site and was therefore excluded from analysis because retrograde tracers would be unlikely to reach the graft. Grafted cells expressed GFP and extended very large numbers of axons for long distances caudal to the lesion site, consistent with previous reports (Figures 5B and 5C; Lu et al., 2012b; Kadoya et al., 2016). Within the graft, large numbers of cells expressed the neuronal marker NeuN (Figures 5F and 5G).

FG injections were present 4–5 mm below the graft, and in no case did FG directly spread from the injection site into the graft (Figure 5A). A mean number of 2,000 ± 382 cells were retrogradely labeled for FG per graft (Figures 5D, 5E, and 6); this number was lower than observed after Cre-mediated retrograde labeling of grafts in mice, likely because the Cre tool was more efficient for detecting retrogradely labeled cells, and also possibly because FG injections into the rat were more caudally located than AAV9-Cre injection in mice. As in mouse studies, there was a distinct skew in the distribution of retrogradely labeled graft neurons toward the caudal half of the NPC graft (Figures 5D–5G). Indeed, quantification revealed that approximately 50% of retrogradely labeled cells in grafts were located within the caudal one-third of the graft (Figure 6). All retrogradely labeled cells in grafts co-localized with NeuN (Figures 5F and 5G).

DISCUSSION

We report here the primary source of the very large numbers of axons that project out from NPC grafts into the distal host spinal cord: neurons that are located in caudal regions of NPC grafts. While monosynaptic projections from host corticospinal neurons to caudally projecting NPC neurons are present, they are found on only 3.9% ± 0.9% of caudally projecting graft neurons (although this number is an underestimate because

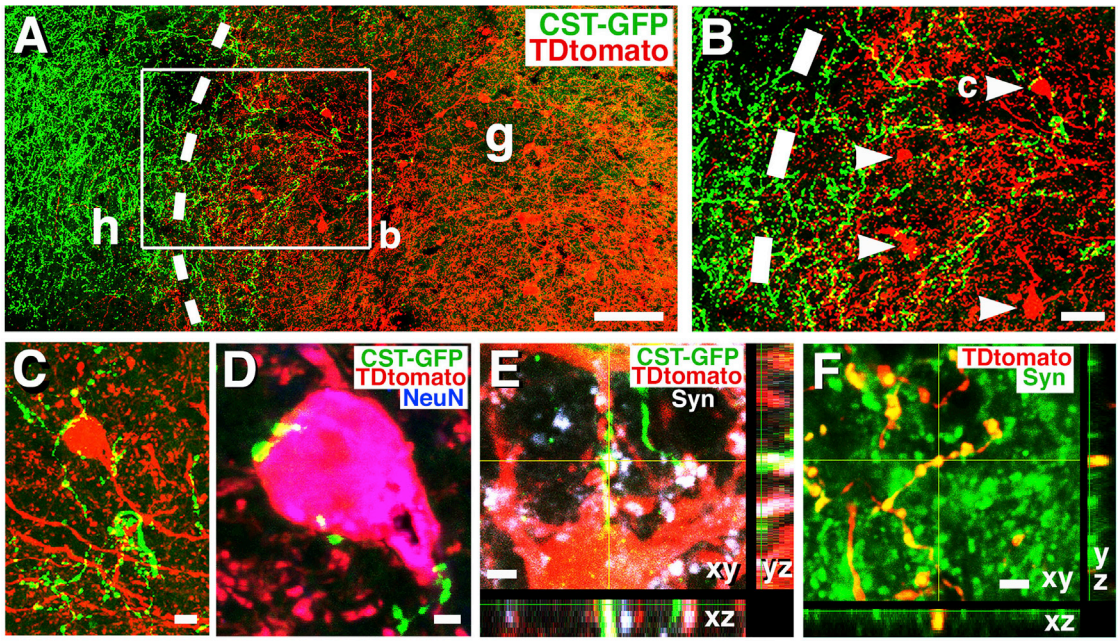

Figure 4. Corticospinal Tract Axonal Regeneration and Connectivity with Caudally Projecting Neurons in Mouse NPC Grafts

(A) Corticospinal tract axons anterogradely labeled with AAV2-GFP injections into the motor cortex regenerate into and converge onto TdTomato-labeled neurons in graft; any TdTomato-labeled neuron in graft must extend an axon to the caudal host spinal cord. Dashed lines indicate host (h)/graft (g) interface. Rostral, left; caudal, right.

(B) Boxed area from (A) shows regenerating corticospinal axons (green) converging on graft neurons (red); these graft neurons extend axons caudal to the lesion site.

(C and D) Corticospinal axons labeled with GFP exhibit bouton-like structures apposed to the soma of TdTomato-expressing neurons that extend axons caudal to the lesion site. Section is also labeled for NeuN in (D).

(E) GFP-labeled corticospinal tract axonal terminals co-localize with the presynaptic marker, synaptophysin (Syn) in apposition to TdTomato-labeled neurons that project caudally.

(F) TdTomato-labeled axonal terminals in caudal gray matter 2 mm from graft express synaptophysin (Syn), suggesting connectivity with host neurons caudal to the lesion.

Scale bars represent 110 μm (A), 70 μm (B), 8 μm (C), 3.5 μm (D), 2.4 μm (E), and 3.5 μm (F).

contacts were only quantified onto graft neuronal somata and not dendrites) (Figure 4). Corticospinal axons and other supraspinal axons typically regenerate into the rostral 0.5–1 mm of a stem cell graft placed in the lesion site (Lu et al., 2012b; Kadoya et al., 2016); were corticospinal axons to project for longer distances through the graft, more monosynaptic projections to grafted neurons that project axons into the distal spinal cord might be formed. One potential means of increasing the distance of host axon regeneration into grafts would be to increase the intrinsic growth state of the host neuron, e.g., by targeting mTOR (mammalian target of rapamycin) pathways (Liu et al., 2010) or enhancing cyclic AMP levels in the host (Lu et al., 2012a; Qiu et al., 2002). Monosynaptic projections from host-to-graft-to-host may be more efficient in supporting functional recovery than polysynaptic projections.

Other host motor axonal systems also project into grafts, including reticulospinal, rubrospinal and serotonergic axons (Adler et al., 2017; Koffler et al., 2018; Lu et al., 2012b; Rosenzweig et al., 2018); however, these axonal systems penetrate only the rostral half of grafts. On the other hand, some host axonal systems, most likely spinal interneurons, penetrate all rostral-caudal levels of NPC grafts, including large grafts placed into monkey spinal cords after injury that measure 4–5 mm in length (Rosenzweig et al., 2018). Recent reports indicate the importance of host interneurons, including propriospinal neurons, in mediating functional improvement after SCI (Chen et al., 2018; Courtine et al., 2008), and future studies will focus on examining connectivity from host spinal interneurons to caudally projecting neurons in grafts.

Why do most axons that project caudally from sites of NPC implantation originate from neurons located in the caudal half of grafts? One simple explanation, supported by Figures 2D, 3A, and 3B, is that axons growing out from neurons in grafts extend radially in all directions.

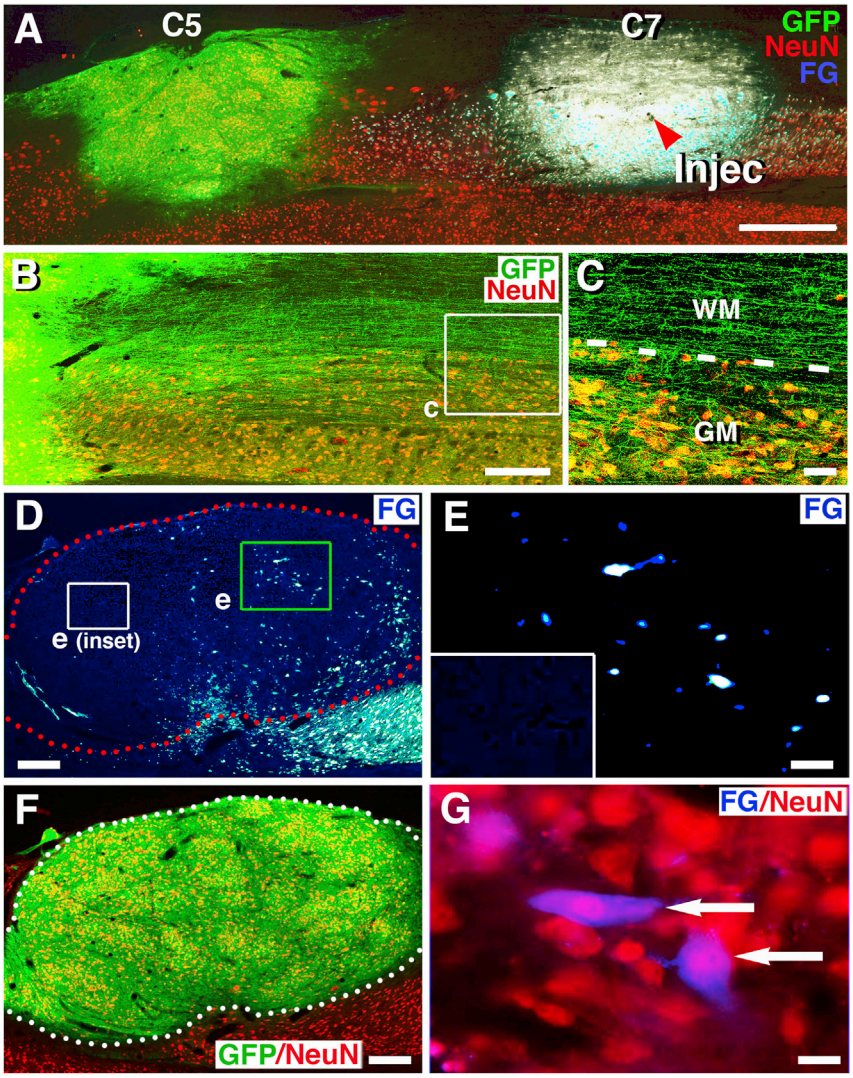

Figure 5. Retrograde Labeling of Caudally Projecting Neurons in Rat NPC Grafts

Rats received GFP-expressing NPC grafts into sites of C5 hemisection, and injections of Fluoro-Gold (FG) into the caudal host spinal cord 3.5 weeks later.

(A) GFP and NeuN immunolabeling reveal graft survival and integration into the lesion site, and the caudal FG injection site at C7 is also visible (arrowhead, Injec). Horizontal section with rostral on left and caudal on right.

(B) GFP and NeuN labeling show extension of large numbers of axons from graft into the caudal host spinal cord.

(C) Numerous axons extend caudal to the lesion site, and axons branch off from white matter (WM) into host gray matter (GM). Dashed lines indicate interface of white matter and gray matter.

(D) Low-magnification view demonstrates numerous cells in NPC graft that are retrogradely labeled with FG. Boxed areas are shown in (E).

(E) A cluster of FG^+ cells in caudal half of graft. Fainter objects are likely cells in partial plane of section; inset shows background in rostral half of graft, which is devoid of FG background labeling.

(F) GFP/NeuN labeling reveals abundant NeuN-expressing cells within the GFP graft shown in (D) and (E).

(G) Two examples (arrows) of FG retrogradely labeled graft cells that co-localize with NeuN, suggesting neuronal identity of retrogradely labeled cells in graft.

Scale bars represent 1,000 μm (A), 210 μm (B), 40 μm (C), 400 μm (D and F), 30 μm (E), and 20 μm (G).

Lacking more specific directional guidance, the neurons most likely to extend axons caudally into the host spinal cord from the graft would be located at the most caudal levels of the graft, where they are most likely to randomly encounter the caudal host spinal cord. It is also possible that molecules diffusing from host to graft could preferentially stimulate axonal outgrowth from more caudally located neurons in the graft (Li et al., 2018; Naoki, 2017), although evidence to support this possibility after SCI in the adult is lacking at present.

Conclusions

The majority of axons extending distally into the host spinal cord from an NPC graft placed in a site of SCI originate from neurons located at caudal levels of the graft. While disynaptic projections from host-to-graft-to-host can be identified, most projections across a graft placed in a site of SCI are likely to be polysynaptic. Future work will focus on increasing the proportion of monosynaptic projections across sites of SCI.

EXPERIMENTAL PROCEDURES

Animals

Both adult C57BL/6 female mice (25–35 g, n = 7, The Jackson Laboratory, Bar Harbor, ME) and female Fischer 344 rats (150–200 g; n = 6, Invigo) were subjects of this study. NIH guidelines for laboratory animal care and safety were strictly followed. The Institutional Animal Care and Use Committee of the Department of Veterans Affairs San Diego Healthcare System approved all animal surgeries. Animals had free access to food and water throughout the study. All surgery was performed under deep anesthesia using

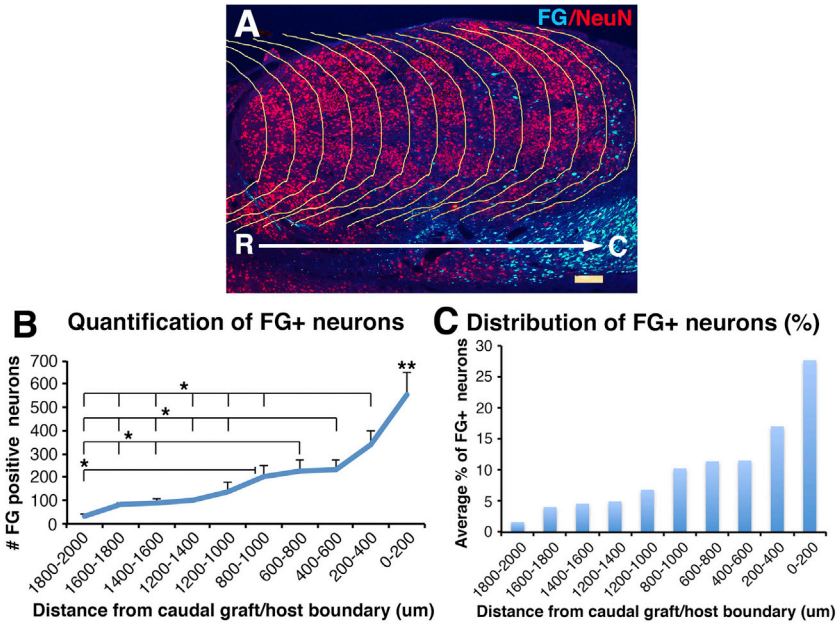

Figure 6. Retrogradely Labeled Neurons in Rat NPC Grafts

(A) NPC graft that double labeled with FG and NeuN was divided into a series of repeating 200-μm regions distributed from the caudal to rostral ends of the graft by superimposing the copied caudal border line for quantification in (B) and (C).

(B) Quantification of total number of FG retrogradely labeled cells at each 200-μm interval along the rostrocaudal extent of the NPC graft. The number of retrogradely labeled cells is significantly greater at caudal levels of the graft (one-way ANOVA, $p < 0.0001$; post hoc Fisher's test, $^{*}p < 0.05$, $^{**}p < 0.01$ comparing 0–200 μm with all other distances). Error bars denote ±SEM. The total mean number of retrogradely labeled neurons in this rat NPC graft is 2,000 ± 382 cells. Greater numbers of retrogradely labeled cells were detected in mouse grafts (Figure 2), presumably due to the greater sensitivity of the Cre-mediated retrograde labeling strategy.

(C) Distribution of FG^{+} neurons in each 200-μm interval as average percentage of total FG^{+} neurons along the rostrocaudal extent of the NPC graft. About 50% of caudally projecting cells are located with the caudal one-third of the graft.

a combination (2 mL/kg) of ketamine (25 mg/mL), xylazine (1.3 g/mL), and acepromazine (0.25 mg/mL).

Neural Progenitor Cell Preparation for Transplantation

Mouse Model

Mouse NPCs were freshly collected from embryonic day 12 (E12) spinal cords of Ai9 mice expressing Cre-dependent TdTomato (B6.CgGt(ROSA)26Sortm9(CAGTdTomato)Hze/J) (Madisen et al., 2010). In the absence of Cre, these NPCs did not express TdTomato (Madisen et al., 2010 and Figure S1). Any grafted cell that received Cre-recombinase would therefore express TdTomato; this occurred in the present study by injecting AAV9-Cre into the caudal host spinal cord, resulting in retrograde Cre transport to the somata of grafted neurons (Figure 1). Freshly dissected E12 spinal cords were placed into 15-mL conical tubes containing 1 mL of ice-cold Hank's balanced salt solution (HBSS). Cells were dissociated chemically with 0.125% trypsin (Harris et al., 2007), and NPCs at a concentration of 250,000 cells/μL were resuspended in fibrin matrices containing a cocktail of three growth factors (vascular endothelial growth factor, brain-derived neurotrophic factor, fibroblast growth factor 2) and calpain inhibitor to promote NPC survival after transplantation, as previously described (Lu et al., 2012b; Robinson and Lu, 2017).

Rat Model

For rat studies, rat E14 spinal cord-derived NPCs from transgenic Fischer 344 rat embryos constitutively expressing GFP under the ubiquitin C promoter (Baska et al., 2008; Bryda et al., 2006) were collected. Freshly dissected E14 spinal cords were placed into 15-mL conical tubes containing 1 mL of ice-cold HBSS. Cells were dissociated chemically with 0.125% trypsin (Harris et al., 2007), and resuspended at a concentration of 250,000 cells/μL in fibrin matrices containing a cocktail of three growth factors and calpain inhibitor as stated above.

Spinal Cord Lesions

C5 lateral hemisection lesions were used in this study because they transect all axonal systems on one-half of the spinal cord, allowing thorough assessment of graft projections to host systems caudal to the injury. The lesion is relatively large, yet animals survive due to sparing of the contralateral half of the spinal cord (Lu et al., 2012b, 2014, 2017). Mice or rats were deeply anesthetized and fixed in a spinal stereotaxy. An incision was made through the cervical dorsal epidermis using a #15 blade. The dorsal muscle tissue was cut to expose the vertebral column and a C5 laminectomy was performed. A small incision was made in the dura along the midline using a scalpel fitted with a #11 blade. A 1-mm block in mice or a 2-mm block in rats of the C5 right-sided spinal cord was cut with iridectomy scissors and removed through microaspiration. Visual inspection of the lesion verified that the entire hemi-cord was removed (Lu et al., 2012b, 2014, 2017). The muscles above the wound were sutured and the skin secured with wound clips. Animals were given daily postoperative injections of lactated Ringer's solution, banamine, and ampicillin for 3 days following surgery.

Cell Transplantation

One week after C5 lateral hemisection surgeries, spinal cords were re-exposed for cell grafting. We chose a 1-week delay for grafting because it is beyond the period of peak acute inflammation

(24–72 h) and a 1-week treatment delay is a clinically relevant time point for potentially treating a stabilized human patient after SCI. Pulled glass micropipettes (outer diameter 80 μm) were filled with 1 μL (for mice) or 2.5 μL (for rats) of the fibrinogen/cell/growth factor solution and, separately, with the 1 μL (mice) or 2.5 μL (rats) of thrombin/cell/growth factor solution. The fibrinogen/growth factor/cell solution was injected gradually into the lesion site over 30 s using a PicoSpritzer II (General Valve, Fairfield, NJ), immediately followed by injection of the thrombin/growth factor/cell solution. The mixing of fibrinogen and thrombin resulted in rapid (<30 s) gelling of the solution in the lesion site to sustain grafted NPCs (Lu et al., 2012b; Robinson and Lu, 2017). The muscles and the skin above the wound were resutured and secured with wound clips, followed by postoperative care as described above.

Retrograde Labeling of Caudally Projecting Graft Neurons

Retrograde Infection of Caudally Projecting Graft Neurons by rAAV-Cre in Mice

For visualization of caudally projecting grafted neurons in mice, we injected 0.5 μL of Cre-recombinase expressing adeno-associated virus 9 (AAV9-CMV-Cre) at a titer of 3×10^{13} particles/mL (University of Pennsylvania) into mouse C7 spinal cord, two spinal cord segments caudal to the graft. AAV9 vectors demonstrate good retrograde transport in the nervous system (Rothermel et al., 2013). Grafted cells express Cre-dependent TdTomato, thus caudal AAV9-Cre injections are expected to result in TdTomato expression in grafted neurons projecting caudally to the sites of AAV9-Cre injection. AAV9-Cre injections into the caudal cord were made 2 weeks post grafting in seven animals using a PicoSpritzer II connected to pulled glass micropipettes with an outer diameter of 40 μm. Injection coordinates targeted central spinal cord gray matter at a depth of 0.5 mm from the dorsal spinal cord surface and 0.4 mm to the right of midline (Figure 1). Injections (100 nL) were made over 1 min and the needle was left in place for an additional minute before slow withdrawal. Muscles were sutured and the skin was closed as described above. Mice survived an additional 2 weeks to allow retrograde infection and expression of TdTomato in grafted neurons, for a total postgraft survival period of 4 weeks. We anticipated that this Cre-dependent mechanism for labeling caudally projecting graft neurons would be more sensitive than retrograde FG injections; this was confirmed (see Results).

Retrograde Labeling of Caudally Projecting Graft Neurons by Fluoro-Gold Injections in Rats

For visualization of caudally projecting graft neurons in rats, we used the retrograde tracer FG rather than AAV9-Cre because Cre-dependent rat donor cell grafts are not available. Rats (n = 6) underwent C5 right lateral hemisection lesions, followed by E14 spinal cord NPC grafts 1 week later. Twenty-five days after grafting, animals received injections of FG in C7 central gray matter (two spinal segments [4–5 mm] caudal to the graft, as in mouse studies), and were sacrificed 3 days later (total survival time 4 weeks post grafting, as in mouse studies). FG (Fluorochrome, Denver, CO) was injected at a concentration of 2.5% in PBS in 150-nL volume. FG was loaded into pulled glass micropipettes (outer diameter 40 μm) and injected at a depth of 1.5 mm from the dorsal spinal cord surface and 0.8 mm to the right of midline (Figure 5) at a rate of 50 nL/min. The needle was left in the injection site for an additional minute and was then slowly withdrawn. Muscles were sutured and the skin closed with wound clips.

Anterograde Tracing of Corticospinal Tract Axons in Mice

To study the association of regenerating CST axons with caudally projecting graft neurons in mice, 1.5 μL of AAV8-GFP (1×10^{13} vector particles/mL, Miami Project Viral Vector Core Facility) was injected into the left motor cortex of three mice to anterogradely label CST axons, 2 weeks post grafting. Injections were placed into four sites at the following coordinates: anterior-posterior coordinates from bregma/mediolateral from midline: 1.0/1.5 mm, 0.5/1.5 mm, −0.5/1.5 mm, −1.0/1.5 mm, all at a depth of 0.5 mm (Liu et al., 2010). Mice survived an additional 2 weeks before sacrifice.

Histology and Immunohistochemistry

One month after grafting, animals were deeply anesthetized and transcardially perfused with ice-cold saline and then 4% paraformaldehyde (PFA). Spinal cords were removed and postfixed in 4% PFA overnight at 4°C. The spinal cords were then cryoprotected in a 30% sucrose solution for 48 h at 4°C. Blocks of spinal cord of 1.5 cm length centered around the graft and AAV9-Cre or FG injection sites were placed into tissue-freezing medium on dry ice. Horizontal sections were cut on a cryostat set at 30-μm intervals and were serially collected into 24-well plates as free-floating sections. Free-floating sections were washed in Tris-buffered saline (TBS) and then incubated for 1 h in TBS containing 5% donkey serum, and 0.25% Triton X-100 to block non-specific binding of antibodies. Sections were then incubated overnight at 4°C in TBS containing 5% donkey serum, 0.25% Triton X-100, and primary antibodies against: RFP (rabbit from Abcam at 1:250, catalog #ab62341) to label grafted mouse cells expressing the Cre-dependent reporter gene, TdTomato; jellyfish GFP (rabbit from Thermo Fisher at 1:1,500, #A-6455) to label grafted cells in rats or CST axons in mice; Cre-recombinase (mouse from BioLegend at 1:100, #900901) to label Cre-recombinase-expressed host cells after AAV9-Cre injection; FG (rabbit from Fluorochrome at 1:1,000, antibodies to FG) to enhance visualization of retrogradely labeled FG-positive neurons, Akhavan et al. (2006); NeuN (mouse from Millipore Sigma at 1:200, #MAB377) to label mature neuronal nuclei; MAP2 (mouse from Millipore Sigma at 1:2,000, #MAB364) to label neuronal soma and dendrites; synaptophysin (mouse from Millipore Sigma at 1:1,000, #MAB5258-I) to label presynaptic terminals; and glial fibrillary acidic protein for astrocytes (goat from Santa Cruz Biotechnology at 1:1500, #Sc-6170). Sections were washed and then incubated at room temperature for 2.5 h with Alexa 488, 594, or 647 conjugated donkey secondary antibodies (Invitrogen at 1:250) along with nuclear stain DAPI (1:1,000). The sections were then washed, mounted on slides, and coverslipped with Fluoromount G (Southern Biotechnology Associates, Birmingham, AL).

Quantification of Caudally Projecting Neurons in Grafts

Mouse Study

The topographical distribution of caudally projecting, TdTomato-expressing neurons in grafts in mice was quantified in every sixth serial horizontal section. Cells were counted that were double labeled for TdTomato and NeuN, in five of seven mice with good graft integration and well-targeted AAV-Cre injection; two subjects were excluded due to poor graft integration in the caudal half of the lesion site. Cells were quantified on digital images of histological sections acquired using a 10× objective (100× total microscopic magnification for source images), and the entire graft was scanned on a Keyance microscope to obtain high-resolution complete images of grafts. Identical exposure settings were used in acquiring all digital images. Only cell somata that were double labeled for TdTomato and the neuronal marker NeuN were counted. The caudal graft border was defined as the edge of continuous and dense TdTomato and NeuN signal, and was traced with the ImageJ Polygon Selection tool as a border line. This caudal border line was then copied and superimposed upon the images at 100-μm intervals moving rostrally to divide the whole graft into a series of repeating 100-μm regions distributed from the caudal border to rostral graft border (i.e., intervals of 0–100 μm, 100–200 μm, 200–300 μm, 300–400 μm, 400–500 μm, 500–600 μm, 600–700 μm, 700–800 μm, 800–900 μm, 900–1,000 μm; Figure 2). The number of TdTomato-expressing neurons that co-labeled with NeuN within each of these 100-μm interval regions was counted manually. TdTomato-expressing neurons lying on lines were only counted within the rostral quantification segment, and were not double counted. The number of TdTomato-labeled neurons from each section was multiplied by a factor of 6, the sampling frequency (1-in-6 sections), to obtain an estimate of total cell number per graft. To quantify the angle at which neurites emerged from caudally projecting neurons, we used sections double labeled for TdTomato and NeuN. A total of 100 neurons double labeled for TdTomato and NeuN were randomly selected within the caudal, middle or rostral one-third of each graft (6–7 neurons per region per animal), and these images were acquired at 400× magnification. Among the 100 sampled neurons, a total of 218 neurite angles were identified. Images were imported into ImageJ and the angle of neurite emergence from the neuronal soma was measured relative to the longitudinal axis of the spinal cord (Figure 3). Circular statistics were used to assess randomness of neurite orientation (see Statistical Analysis).

Rat Study

The topographical distribution of caudally projecting, FG-labeled neurons in grafts in rats was quantified in every sixth serial horizontal section. Sections were triple labeled for GFP, FG, and NeuN. Cells were counted in four of six rats with good graft integration and well-targeted FG injections; one subject was excluded due to poor graft integration in the caudal half of the lesion site, and the other subject had mistargeting of the FG injection predominantly into the right lateral white matter. Cells were quantified on digital images of histological sections acquired using a 10× objective (100× total microscopic magnification for source images), and the entire graft was scanned on a Keyance microscope. Identical exposure settings were used to acquire all images. Only cell somata that double labeled for FG and the neuronal marker NeuN were counted. The caudal graft border was defined as the edge of continuous, dense, and homogeneous GFP and NeuN signal and was traced with the ImageJ Polygon Selection tool as a border line. This caudal border line was then copied and superimposed upon the images at 200-μm intervals rostrally to divide the whole graft into a series of repeating 200-μm regions distributed from the caudal border to rostral graft border (i.e., 0–200 μm, 200–400 μm, 400–600 μm, 600–800 μm, 800–1,000 μm, 1,000–1,200 μm, 1,200–1,400 μm, 1,400–1,600 μm, 1,600–1,800 μm, 1,800–2,000 μm etc.; Figures 5 and 6); 200-μm intervals were used in the rat compared with 100-μm intervals in the mouse because the rat grafts were larger. The number of FG-labeled neurons that co-labeled with NeuN within each of these 200-μm interval regions was counted manually. FG-labeled cells lying on lines were only counted within the rostral quantification segment and were not double counted. The number of FG-labeled neurons from each section was multiplied by a factor of 6, the sampling frequency (1-in-6 sections), to obtain an estimate of total cell number per graft.

Statistical Analysis

Quantification could not be performed in a blinded manner because there was only one treatment group, and differences in mouse and rat spinal cord sizes were obvious on inspection. For assessing neuronal numbers, multiple quantification regions were compared by ANOVA (JMP software) at a designated significance level of $p < 0.05$, followed by Fisher's post hoc tests between individual quantified segments. Data are presented as mean ± SEM. For assessment of the angle of neurite emergence from grafted neurons, circular statistics were used: the Walker-Watson test was used as a non-parametric test of group mean for circular data, then Rayleigh's test examined the null hypothesis that all angles were uniformly distributed around a 360° axis, using a significance criterion of $p < 0.05$.

SUPPLEMENTAL INFORMATION

Supplemental Information can be found online at https://doi.org/10.1016/j.stemcr.2019.05.011.

AUTHOR CONTRIBUTIONS

P.L. designed and carried out *in vivo* experiments, interpreted results, and wrote the manuscript. W.G.L. contributed immunohistochemistry, quantification, and project design. S.N. contributed to surgery, quantification, and project design. G.D. contributed to neurite angle measurement and quantification. J.R.H. and A.R.F. contributed to statistical analysis. L.G. contributed to *in vivo* experiments. M.H.T. contributed to project design, data interpretation, and writing of the manuscript.

ACKNOWLEDGMENTS

This work was supported by the Veterans Administration (Gordon Mansfield Collaborative Consortium [1I50RX001706-01] and Merit Review grants [1 I01 BX001252-01A2 and 1 I21 RX00084-01A1]), NIH (1 I01 BX001252-01A2, NS09881, and EB014986),

the Craig H. Neilsen Foundation, the California Institute for Regenerative Medicine, the Dr. Miriam and Sheldon G. Adelson Medical Research Foundation, and the Bernard and Anne Spitzer Charitable Trust. W.G.-L. was a recipient of a fellowship from CNPQ-Brazil.

Received: October 10, 2018
Revised: May 10, 2019
Accepted: May 12, 2019
Published: June 13, 2019

REFERENCES

Adler, A.F., Lee-Kubli, C., Kumamaru, H., Kadoya, K., and Tuszynski, M.H. (2017). Comprehensive monosynaptic rabies virus mapping of host connectivity with neural progenitor grafts after spinal cord injury. Stem Cell Reports *8*, 1525–1533.

Akhavan, M., Hoang, T.X., and Havton, L.A. (2006). Improved detection of Fluorogold labeled neurons in long-term studies. J. Neurosci. Methods *152*, 156–162.

Baska, K.M., Manandhar, G., Feng, D., Agca, Y., Tengowski, M.W., Sutovsky, M., Yi, Y.J., and Sutovsky, P. (2008). Mechanism of extracellular ubiquitination in the mammalian epididymis. J. Cell Physiol. *215*, 684–696.

Berry, M.S., and Pentreath, V.W. (1976). Criteria for distinguishing between monosynaptic and polysynaptic transmission. Brain Res. *105*, 1–20.

Bonner, J.F., Connors, T.M., Silverman, W.F., Kowalski, D.P., Lemay, M.A., and Fischer, I. (2011). Grafted neural progenitors integrate and restore synaptic connectivity across the injured spinal cord. J. Neurosci. *31*, 4675–4686.

Bryda, E.C., Pearson, M., Agca, Y., and Bauer, B.A. (2006). Method for detection and identification of multiple chromosomal integration sites in transgenic animals created with lentivirus. Biotechniques *41*, 715–719.

Chen, B., Li, Y., Yu, B., Zhang, Z., Brommer, B., Williams, P.R., Liu, Y., Hegarty, S.V., Zhou, S., Zhu, J., et al. (2018). Reactivation of dormant relay pathways in injured spinal cord by KCC2 manipulations. Cell *174*, 521–535.e13.

Courtine, G., Song, B., Roy, R.R., Zhong, H., Herrmann, J.E., Ao, Y., Qi, J., Edgerton, V.R., and Sofroniew, M.V. (2008). Recovery of supraspinal control of stepping via indirect propriospinal relay connections after spinal cord injury. Nat. Med. *14*, 69–74.

Haas, C., and Fischer, I. (2014). Transplanting neural progenitors to build a neuronal relay across the injured spinal cord. Neural Regen. Res. *9*, 1173–1176.

Harris, J., Lee, H., Tu, C.T., Cribbs, D., Cotman, C., and Jeon, N.L. (2007). Preparing e18 cortical rat neurons for compartmentalization in a microfluidic device. J. Vis. Exp., 305. https://doi.org/10.3791/305.

Kadoya, K., Lu, P., Nguyen, K., Lee-Kubli, C., Kumamaru, H., Yao, L., Knackert, J., Poplawski, G., Dulin, J.N., Strobl, H., et al. (2016). Spinal cord reconstitution with homologous neural grafts enables robust corticospinal regeneration. Nat. Med. *22*, 479–487.

Koffler, J., Zhu, W., Qu, X., Platoshyn, O., Dulin, J., Brock, J., Graham, L., Lu, P., Sakamoto, J., Marsala, M., et al. (2018). Biomimetic 3D printed spinal cord scaffolds for 1 spinal cord injury. Nat. Med. *25*, 263–269.

Kumamaru, H., Kadoya, K., Adler, A.F., Takashima, Y., Graham, L., Coppola, G., and Tuszynski, M.H. (2018). Generation and post-injury integration of human spinal cord neural stem cells. Nat. Methods *15*, 723–731.

Li, Q., Yang, C., Zhang, B., Guo, Z., and Lin, J. (2018). Wnt3a ectopic expression interferes axonal projection and motor neuron positioning during the chicken spinal cord development. J. Mol. Neurosci. *64*, 619–630.

Liu, K., Lu, Y., Lee, J.K., Samara, R., Willenberg, R., Sears-Kraxberger, I., Tedeschi, A., Park, K.K., Jin, D., Cai, B., et al. (2010). PTEN deletion enhances the regenerative ability of adult corticospinal neurons. Nat. Neurosci. *13*, 1075–1081.

Lu, P., Wang, Y., Graham, L., McHale, A.K., Gao, M., Wu, D., Brock, J., Blesch, A., Rosenzweig, E., Havton, L., et al. (2012a). Long-distance growth and connectivity of neural stem cells after severe spinal cord injury. Cell *150*, 1264–1273.

Lu, P., Blesch, A., Graham, L., Wang, Y., Samara, R., Banos, K., Haringer, V., Havton, L., Weishaupt, N., Bennett, D., et al. (2012b). Motor axonal regeneration after partial and complete spinal cord transection. J. Neurosci. *32*, 8208–8218.

Lu, P., Woodruff, G., Wang, Y., Graham, L., Wu, D., Poplawski, G., Brock, J., Goldstein, L., and Tuszynski, T. (2014). Long-distance axonal growth of neural stem cells derived from human induced pluripotent stem cells after spinal cord injury. Neuron *83*, 789–796.

Lu, P., Ceto, S., Wang, Y., Graham, L., Wu, D., Kumamaru, H., Staufenberg, E., and Tuszynski, M.H. (2017). Prolonged human neural stem cell maturation supports recovery in injured rodent CNS. J. Clin. Invest. *127*, 3287–3299.

Madisen, L., Zwingman, T.A., Sunkin, S.M., Oh, S.W., Zariwala, H.A., Gu, H., Ng, L.L., Palmiter, R.D., Hawrylycz, M.J., Jones, A.R., et al. (2010). A robust and high-throughput Cre reporting and characterization system for the whole mouse brain. Nat. Neurosci. *13*, 133–140.

Naoki, H. (2017). Revisiting chemoaffinity theory: chemotactic implementation of topographic axonal projection. PLoS Comput. Biol. *13*, e1005702.

Qiu, J., Cai, D., Dai, H., McAtee, M., Hoffman, P.N., Bregman, B.S., and Filbin, M.T. (2002). Spinal axon regeneration induced by elevation of cyclic AMP. Neuron *34*, 895–903.

Robinson, J., and Lu, P. (2017). Optimization of trophic support for neural stem cell grafts in sites of spinal cord injury. Exp. Neurol. *291*, 87–97.

Rosenzweig, E.S., Brock, J.H., Lu, P., Kumamaru, H., Salegio, E.A., Kadoya, K., Weber, J.L., Liang, J.J., Moseanko, R., Hawbecker, S., et al. (2018). Restorative effects of human neural stem cell grafts on the primate spinal cord. Nat. Med. *24*, 484–490.

Rothermel, M., Brunert, D., Zabawa, C., Díaz-Quesada, M., and Wachowiak, M. (2013). Transgene expression in target-defined neuron populations mediated by retrograde infection with adeno-associated viral vectors. J. Neurosci. *33*, 15195–15206.